

THE EXPLOITATION OF THE NON LOCAL PARADIGM FOR SAR 3D RECONSTRUCTION

Giampaolo Ferraioli, Loïc Denis, Charles-Alban Deledalle, Florence Tupin

▶ **To cite this version:**

Giampaolo Ferraioli, Loïc Denis, Charles-Alban Deledalle, Florence Tupin. THE EXPLOITATION OF THE NON LOCAL PARADIGM FOR SAR 3D RECONSTRUCTION. IGARSS (International Geoscience and Remote Sensing Symposium), Jul 2019, Yokohama, Japan. hal-02374544

HAL Id: hal-02374544

https://telecom-paris.hal.science/hal-02374544

Submitted on 21 Nov 2019

HAL is a multi-disciplinary open access archive for the deposit and dissemination of scientific research documents, whether they are published or not. The documents may come from teaching and research institutions in France or abroad, or from public or private research centers.

L'archive ouverte pluridisciplinaire **HAL**, est destinée au dépôt et à la diffusion de documents scientifiques de niveau recherche, publiés ou non, émanant des établissements d'enseignement et de recherche français ou étrangers, des laboratoires publics ou privés.

THE EXPLOITATION OF THE NON LOCAL PARADIGM FOR SAR 3D RECONSTRUCTION

Giampaolo Ferraioli[(1)], *Loic Denis*[(2)], *Charles-Alban Deledalle*[(3)], *Florence Tupin*[(4)]

[(1)]Dipartimento di Scienze e Tecnologie
Università degli Studi di Napoli "Parthenope" – Naples, Italy
[(2)]CNRS-Univ. Saint-Etienne, Laboratoire Hubert Curien – Saint-Etienne, France
[(3)]CNRS-Univ. Bordeaux, IMB – Talence, France
[(4)]LTCI, Télécom ParisTech, Université Paris-Saclay, – Paris, France

ABSTRACT

In the last decades, several approaches for solving the Phase Unwrapping (PhU) problem using multi-channel Interferometric Synthetic Aperture Radar (InSAR) data have been developed. Many of the proposed approaches are based on statistical estimation theory, both classical and Bayesian. In particular, the statistical approaches based on the use of the whole complex multi-channel dataset have turned to be effective. The latter are based on the exploitation of the covariance matrix, which contains the parameters of interest. In this paper, the added value of the Non Local (NL) paradigm within the InSAR multi-channel PhU framework is investigated. The analysis of the impact of NL technique is performed using multi-channel realistic simulated data and X-band data.

Index Terms— SAR Interferometry, Phase Unwrapping, Multi-channel, Non Local Paradigm

1. INTRODUCTION

Synthetic Aperture Radar Interferometry (InSAR) is a powerful technique able to provide the height of the observed scene. The main aspects that limit the application of this technique for the generation of the Digital Elevation Models (DEM) are the presence of noise and the wrapped nature of the acquired phase data. In particular, the combination of these two effects makes the height retrieval problem an ill-posed one. In particular, when the absolute value of interferometric phase difference between neighboring pixels exceeds π, the obtained solution is ambiguous [1], [2]. It is, therefore, necessary to exploit more data in order to restore the uniqueness of the solution and to provide the height estimation. Multi-channel (MC) interferometry has turned to be an effective instrument for this aim. In MC Interferometry multiple interferograms acquired with different channels (baselines or frequencies) are jointly exploited [3], [4].
In the last fifteen years several multi-channel algorithms have been presented [5], [6], [7], [8]. Among multi-channel techniques, algorithms based on the exploitation of the whole complex dataset have shown interesting and effective results [9]. The idea is to model jointly all channels of the MC SAR image: instead of marginalizing the data distribution with respect to missing parameters the joint distribution of the data can be used. Within this framework, the estimation of the covariance assumes a fundamental role. Usually it is estimated using a limited number of samples, selected in a local neighbor of the considered pixel, as it happens in boxcar based approaches. However several limitations of such an estimation are known, such as loss of resolution. A robust estimation of the covariance matrix, provided by the NL paradigm could provide an added value. In this paper, the analysis of the impact of NL technique on the multi-channel PhU reconstruction problem is performed. The use of NL approach for 3D reconstruction within classical and Bayesian estimation theory PhU algorithm is addressed. A comparison with the classical boxcar-averaging approach is reported and results are discussed and evaluated. In order to quantitatively compare the different algorithms and to highlight the peculiarity of each approach, a testing scenario is constructed. Finally, a qualitative analysis is conducted on real X-band data.

2. METHODS

In this section different methods for multi-channel PhU based on the whole complex data are briefly described. For all the considered methods, the notation is the following: D is the number of available channels (i.e. baselines), i designates one of the N pixels of the image, a and b are two channels among the D channels, λ is the working wavelength,$\gamma_{a,b}$ is the coherence coefficient, $B_\perp(a,b)$ is the orthogonal baseline between channels a and b, ρ_0 is the distance to the scene, and θ is the view angle.

2.1. ML estimator

The first method presented is the classical Maximum Likelihood (ML) one [9].

The measured values are collected in the vector $\boldsymbol{g}_i$ of D complex values. The statistical distribution of $\boldsymbol{g}_i$ for the pixel i, under the hypothesis of fully developed speckle is given by a complex circular Gaussian distribution:

$$\mathrm{p}(\boldsymbol{g}_i|\boldsymbol{\Sigma}_i) = \frac{1}{\pi^D \det(\boldsymbol{\Sigma}_i)} \exp\left(-\boldsymbol{g}_i^\dagger \, \boldsymbol{\Sigma}_i^{-1} \, \boldsymbol{g}_i\right) \tag{1}$$

with $\dagger$ the Hermitian transpose operator and $\boldsymbol{\Sigma}_i$ is the complex covariance matrix at pixel i which depends on the radiometry R, the inter-channel coherence $\gamma_{a,b}$ and the interferometric phases $\psi_{a,b}$, previously defined. The latter is related to the height h by a well known relation, that accounts for the interferometric baseline, possible atmospheric distortions and other calibration parameters. The Maximum Likelihood (ML) estimator of the height can be obtained as:

$$\hat{\mathbf{h}} = \arg\max_{\mathbf{h}} \quad \mathrm{p}(\boldsymbol{g}_i|\boldsymbol{\Sigma}_i) \tag{2}$$

In order to perform the maximization, an estimation of the covariance matrix $\boldsymbol{\Sigma}_i$ is needed. A simple boxcar filter could be applied. The estimation of $\boldsymbol{\Sigma}_i$ is obtained by spatial averaging over a square window centered on the considered pixel.

2.2. ML-NL estimator

The previous approach suffers of one main drawback: the covariance estimation involves an averaging procedure that degrades the spatial resolution by blurring thin structures. It can be interesting to include in the estimation of $\boldsymbol{\Sigma}_i$ not the neighboring pixels, but the similar ones. In other words, the covariance matrix could be estimated by using the similar pixels found across the whole image. The estimated covariance matrix can thus be obtained as:

$$\boldsymbol{\Sigma}_i^{(\mathrm{NL})} = \frac{1}{\sum_j \omega_{i,j}} \sum_j \omega_{i,j} \; \boldsymbol{g}_j \, \boldsymbol{g}_j^\dagger \tag{3}$$

where $\omega_{i,j}$ are the non-local coefficients that balance the weight of observations $\boldsymbol{g}_j$ at pixel j according to their relevance for the estimation at pixel i. It is clear that the choice of the weights is crucial. We chose to compute the weights using the NL-SAR algorithm [10], which has shown interesting performances.

2.3. MAP estimator

Moving to Bayesian estimation theory, the contextual information is added to the likelihood function. The idea is to model the unknown parameters by using an a priori statistical distribution, which takes into account the correlation between each pixel and its neighborhood. An effective tool to statistically describe and model the unknown image is the Markov random field (MRF). In particular we adopt the Total Variation (TV) energy model. The Maximum a Posteriori solution is given by adding the TV energy model to the logarithm of the likelihood term of Eq. (1). In particular:

$$\hat{\mathbf{h}} = \arg\min_{\mathbf{h}} [-\log \mathrm{p}(\boldsymbol{g}_i|\boldsymbol{\Sigma}_i) + \mathrm{TV}(\mathbf{h})], \tag{4}$$

Again, in order to perform the maximization, an estimation of the covariance matrix $\boldsymbol{\Sigma}_i$ is needed. A simple boxcar filter could be applied.

2.4. MAP-NL estimator

Following the ML-NL approach, the maximum a posteriori estimator can be modified taking into account the similarity between pixels. In particular, the similarity is exploited for the estimation of the covariance matrix $\boldsymbol{\Sigma}_i$ at each pixel using NL-SAR method [10]. Using this approach, and by making some simple considerations the function of Eq. (4) can be simplified into an easier expression, providing the Patch-based estimation and regularized inversion for multi-baseline SAR interferometry (PARISAR) estimator proposed in [11].

3. TESTING FRAMEWORK

The four previously presented techniques have been compared on both simulated and real dataset. Concerning the simulated dataset, the scenario consists of 6 buildings with different heights and shapes (see Fig.1 - True Profile). Three complex images have been simulated starting from the True Profile and the mean coherence map (see Fig.1 - Coherence). In order to make it more realistic, the data have been simulated considering different coherence values, including shadowing ones. Two of the three available interferograms are shown in the first line of Fig.1. Concerning the optimization step, a graph-cut algorithm using Ishikawa's construction is adopted for all the considered algorithms. The results of the previously reported methods are shown in the second line of Fig.1. The added value of the NL apporach is evident for both ML-NL and MAP-NL, compared to ML and MAP, respectively. The effectiveness of the exploitation of similar pixels for the estimation of the covariance matrix, and consequently for the 3D reconstruction is evident.

The four methods have also been tested on a real dataset. This dataset is composed of three COSMO-SkyMed Stripmap images acquired close to Nola. In the first row of Figure 2 the data (interferograms) are reported together with the mean coherence. In the second row the estimations using ML,ML-NL, MAP and MAP-NL are shown. Again the effectiveness of the NL apporach is evident.

In the final version of the paper a quantitative analysis based on computational time, memory complexity and accuracy will be carried out, together with a qualitative analysis based on in situ optical images of the observed Nola area.

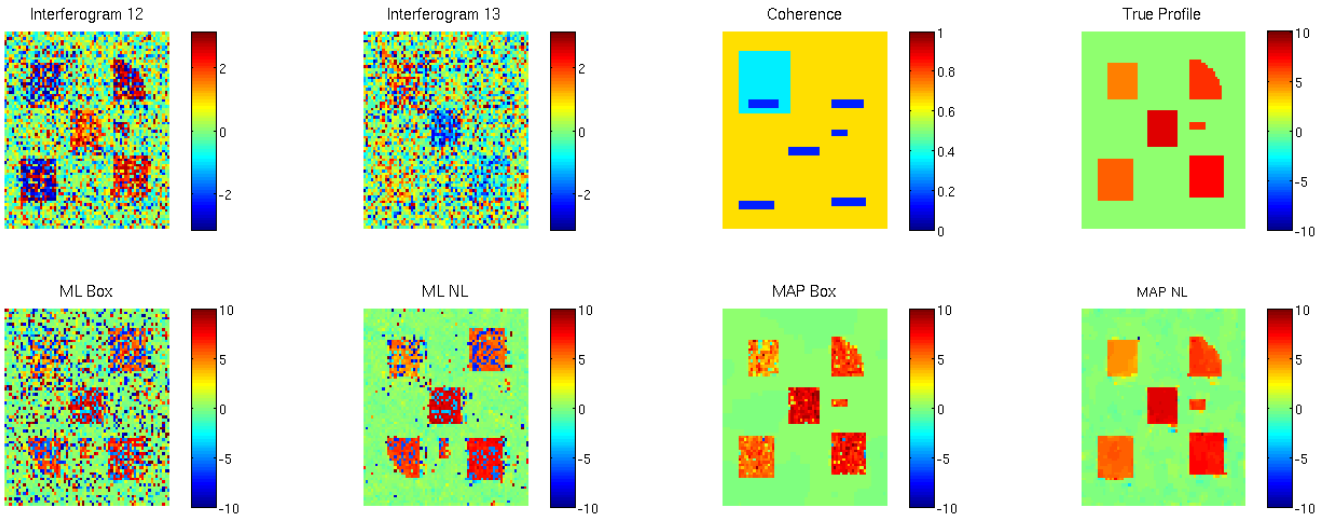


Fig. 1. Simulated Dataset. First row: interferograms and true profile. Second row: results using different approaches.

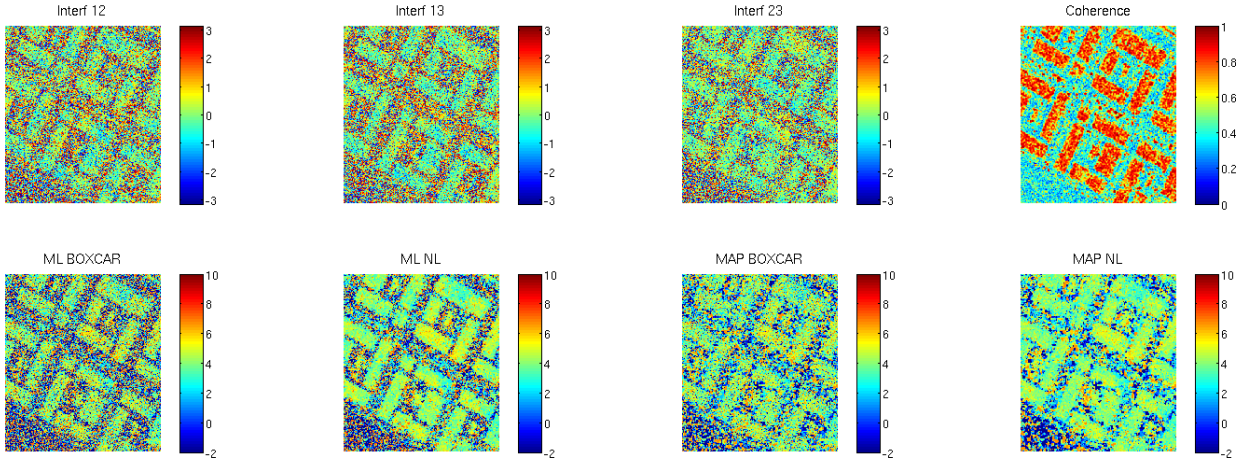


Fig. 2. Real Dataset. First row: interferograms and coherence image. Second row: results using different approaches.

4. REFERENCES

[1] J.M. Bioucas-Dias and G. Valadao, "Phase unwrapping via graph cuts," *Image Processing, IEEE Transactions on*, vol. 16, no. 3, pp. 698–709, 2007.

[2] Runpu Chen, Weidong Yu, R. Wang, Gang Liu, and YunFeng Shao, "Integrated Denoising and Unwrapping of InSAR Phase Based on Markov Random Fields," *IEEE Transactions on Geoscience and Remote Sensing*, vol. 51, no. 8, pp. 4473–4485, Aug 2013.

[3] G. Fornaro, A. Pauciullo, and E. Sansosti, "Phase difference-based multichannel phase unwrapping," *Image Processing, IEEE Transactions on*, vol. 14, no. 7, pp. 960–972, 2005.

[4] M. Eineder and N. Adam, "A maximum-likelihood estimator to simultaneously unwrap, geocode, and fuse SAR interferograms from different viewing geometries into one digital elevation model," *IEEE Transactions on Geoscience and Remote Sensing*, vol. 43, no. 1, pp. 24–36, 2005.

[5] M. Schmitt and U. Stilla, "Maximum-likelihood estimation for multi-aspect multi-baseline SAR interferometry of urban areas," *ISPRS Journal of Photogrammetry and Remote Sensing*, vol. 87, no. 0, pp. 68 – 77, 2014.

[6] H. Liu, M. Xing, and Z. Bao, "A Cluster-Analysis-

Based Noise-Robust Phase-Unwrapping Algorithm for Multibaseline Interferograms," *IEEE Transactions on Geoscience and Remote Sensing*, vol. 53, no. 1, pp. 494–504, 2015.

[7] D. Chirico and G. Schirinzi, "Multichannel interferometric SAR phase unwrapping using extended Kalman Smoother," *International Journal of Microwave and Wireless Technologies*, vol. 5, pp. 429–436, 6 2013.

[8] B. Osmanoglu, T.H. Dixon, and S. Wdowinski, "Three-dimensional phase unwrapping for satellite radar interferometry, i: Dem generation," *Geoscience and Remote Sensing, IEEE Transactions on*, vol. 52, no. 2, pp. 1059–1075, Feb 2014.

[9] F. Baselice, A Budillon, G. Ferraioli, V. Pascazio, and G. Schirinzi, "Multibaseline SAR Interferometry from Complex Data," *IEEE Journal of Selected Topics in Applied Earth Observations and Remote Sensing*, vol. 7, no. 7, pp. 2911–2918, July 2014.

[10] Charles-Alban Deledalle, Loïc Denis, Florence Tupin, Andreas Reigber, and Marc Jäger, "NL-SAR: A unified nonlocal framework for resolution-preserving (Pol)(In) SAR denoising," *IEEE Transactions on Geoscience and Remote Sensing*, vol. 53, no. 4, pp. 2021–2038, 2015.

[11] G. Ferraioli, C. A. Deledalle, L. Denis, and F. Tupin, "PARISAR: Patch-Based Estimation and Regularized Inversion for Multibaseline SAR Interferometry," *IEEE Transactions on Geoscience and Remote Sensing*, vol. PP, no. 99, pp. 1–11, 2017.